



Radioactive Beams in Particle Therapy: Past, Present, and Future

Marco Durante^{1,2*} and Katia Parodi³

¹ Biophysics Department, GSI Helmholtzzentrum für Schwerionenforschung, Darmstadt, Germany, ² Institute of Condensed Matter Physics, Technische Universität Darmstadt, Darmstadt, Germany, ³ Department of Experimental Physics—Medical Physics, Ludwig-Maximilians-Universität München, Munich, Germany

Heavy ion therapy can deliver high doses with high precision. However, image guidance is needed to reduce range uncertainty. Radioactive ions are potentially ideal projectiles for radiotherapy because their decay can be used to visualize the beam. Positron-emitting ions that can be visualized with PET imaging were already studied for therapy application during the pilot therapy project at the Lawrence Berkeley Laboratory, and later within the EULIMA EU project, the GSI therapy trial in Germany, MEDICIS at CERN, and at HIMAC in Japan. The results show that radioactive ion beams provide a large improvement in image quality and signal-to-noise ratio compared to stable ions. The main hindrance toward a clinical use of radioactive ions is their challenging production and the low intensities of the beams. New research projects are ongoing in Europe and Japan to assess the advantages of radioactive ion beams for therapy, to develop new detectors, and to build sources of radioactive ions for medical synchrotrons.

OPEN ACCESS

Edited by:

Claudia Kuntner,
Austrian Institute of Technology
(AIT), Austria

Reviewed by:

Bruno Golosio,
University of Cagliari, Italy
Timothy DeGrado,
Mayo Clinic, United States

*Correspondence:

Marco Durante
m.durante@gsi.de

Specialty section:

This article was submitted to
Medical Physics and Imaging,
a section of the journal
Frontiers in Physics

Received: 25 April 2020

Accepted: 14 July 2020

Published: 28 August 2020

Citation:

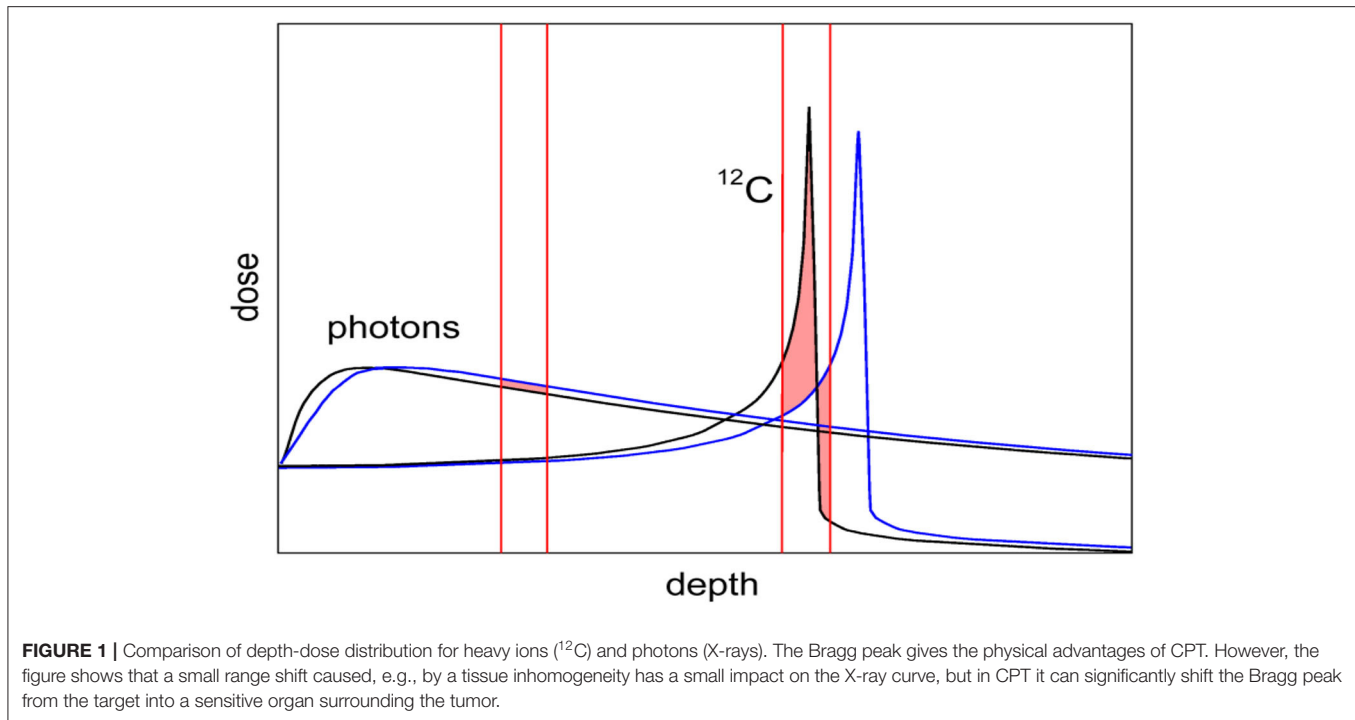
Durante M and Parodi K (2020)
Radioactive Beams in Particle
Therapy: Past, Present, and Future.
Front. Phys. 8:326.
doi: 10.3389/fphy.2020.00326

Keywords: particle therapy, radioactive ion beams, carbon ions, oxygen ions, PET

INTRODUCTION

Currently, ~50% of cancer patients in Europe experience radiotherapy, generally by X-rays, as part of their treatment [1]. In recent years, photon radiotherapy has greatly improved its accuracy and safety thanks to image guidance (IGRT) [2]. However, charged particle therapy (CPT) with protons and light ions is rapidly growing all over the world, particularly in Europe [3]. In fact, thanks to the favorable depth-dose distribution, more normal tissue is spared with CPT compared to conventional radiotherapy with X-rays in virtually all sites, leading to high success/toxicity ratios [4]. Using ions heavier than protons, generally carbon ions, the physics advantages are added to the radiobiological properties, being stopping (high-LET) ions in the tumor region more effective than X-rays or protons for cell killing, while in the normal tissue, fast (low-LET) ions induce a toxicity comparable to sparsely ionizing radiation [5]. The experience at the National Institute of Radiological Sciences (NIRS) in Chiba (Japan) [6] and in the European centers [7] demonstrates that the radiobiological and physical rationale is actually translated in improved clinical results for several indications [8].

Yet, CPT remains controversial [9]. The first reason is the higher cost of the CPT facilities [10], especially the expensive heavy ion centers. Even if the cost is still much higher for particle therapy centers compared to linacs for X-rays, it is declining, mostly thanks to superconductive technologies now employed for the construction of the accelerators (cyclotrons, synchro-cyclotrons, or synchrotrons) [11, 12]. However, CPT is also limited in what should be the main advantage, i.e., the high precision made possible by the Bragg peak. CPT is indeed less robust than conventional radiotherapy because of considerable uncertainty on the particle range and poor image guidance [13]. While the lateral penumbra is shallower for protons than for X-rays, making the proton plans



robust for misalignments in the direction orthogonal to the beam direction [14], for heavy ions, characterized by sharp dose gradients in all directions and very high doses in the distal ends, range uncertainty is the main physics limitation. Image guidance is essential for CPT, even more so than for X-rays, because a shift in the Bragg peak has a much larger impact on the dose than for photons (**Figure 1**). For moving targets this also occurs through the interplay effect, causing underdosage to part of the target [15]. In-room CT and cone-beam CT are emerging as the two image guidance methods of choice for CPT, but IGRT using X-rays is more accurate and robust [16] and is quickly improving thanks to the recent introduction of online magnetic resonance imaging (MRI) [17, 18]. Clinically, a substantial margin is added in CPT to the prescribed range in order to ensure tumor coverage, e.g., in proton therapy, this range margin is on the order of 3.5% of the prescribed range [19]. Wide margins jeopardize one of the main advantages of the Bragg peak: the steep dose gradients and the potential high accuracy and precision [20].

To tackle the range uncertainty problem, several methods for range verification have been developed. Imaging in radiology very often uses radioactive tracers, and it was indeed proposed already long ago [21] that radioactive ion beams (RIB) have the potential for simultaneous treatment and beam visualization, similar to theranostics with radioisotopes [22]. We will first describe the current methods for heavy ion beam visualization, and then the past experience is using RIB in cancer therapy. We will then argue that the current efforts for high-intensity accelerators can lead to a more effective use of RIB in therapy, pending experimental proof of the clinical advantages.

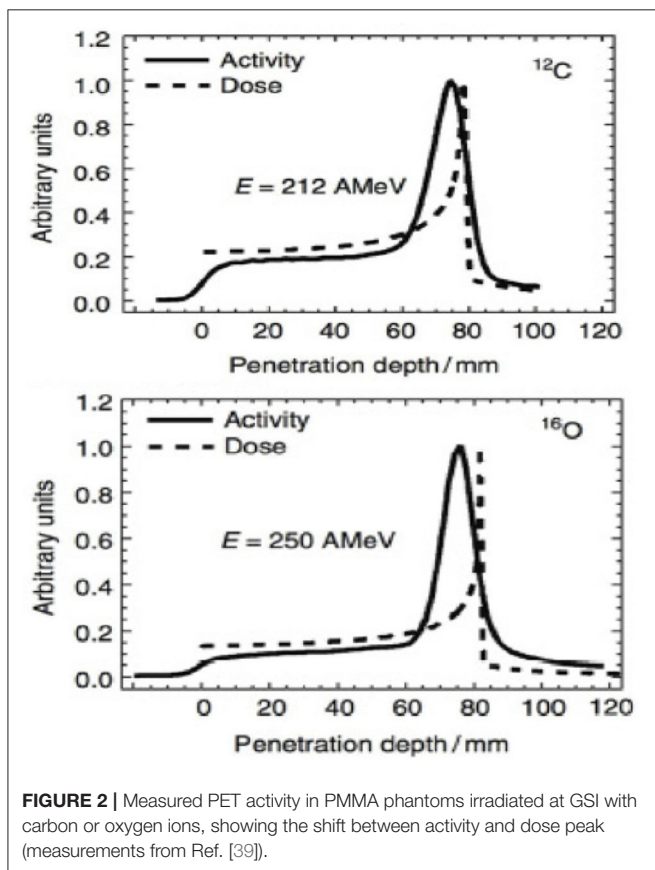
RANGE VERIFICATION IN PARTICLE THERAPY

Even if image guidance is less common in CPT compared to conventional radiotherapy, the physics of charged particles offers unique opportunities for *in vivo* range verification. In proton therapy, there is an increasing use of prompt γ -ray detectors that measure the emission of photons by nuclear reactions and their fast decay shortly before the Bragg peak [23]. The method has been tested also for high-energy C-ions in phantoms [24, 25]. Several other methods have been proposed, such as ionoacoustic measurements [26] or mixed beams [27]. For C-ions, it is also possible to measure secondary charged particles, such as protons emitted at large angles [28, 29]. A combination of different methods is under study for animal irradiators [30] and in clinical settings [31, 32]. Reviews of different methods for *in vivo* range verification can be found in Refs. [33–36].

The range verification method that has been tested most extensively in clinical practice is positron emission tomography (PET) [37]. PET is a well-known diagnostic imaging method, based on the detection of the two 511 keV photons emitted by annihilation of a positron with an electron in the media. Unlike conventional diagnostic imaging [38], currently PET in particle therapy exploits β^+ -emitting isotopes produced by the particle beam in the patient's body by nuclear fragmentation [37]. In proton therapy, only target fragments can be used for imaging, while in heavy ion therapy, the projectile fragments provide a large part of the signal with better correlation to the dose. A list of typical radionuclides produced by target fragmentation in proton therapy or potential projectile fragments is provided in **Table 1**. The radioactive projectile fragments provide a peak in the activity

TABLE 1 | Positron-emitting isotopes that are found in proton therapy by target fragmentation and/or that have been considered as projectiles for RIB therapy.

Stable isotope	Positron-emitting isotopes	Half-life
^{12}C	^{11}C	20.33 min
	^{10}C	19.3 s
^{14}N	^{13}N	9.97 min
	^{12}N	11.0 ms
^{16}O	^{15}O	2.04 min
	^{14}O	1.17 min
^{19}F	^{18}F	1.83 h
	^{17}F	1.07 min
^{20}Ne	^{19}Ne	17.26 s
	^{18}Ne	1.66 s
^{31}P	^{30}P	2.50 min
	^{29}P	4.14 s

**FIGURE 2** | Measured PET activity in PMMA phantoms irradiated at GSI with carbon or oxygen ions, showing the shift between activity and dose peak (measurements from Ref. [39]).

that is not observed in proton therapy (Figure 2) [40]. However, the activity peak invariably occurs upstream of the Bragg peak, because the light isotopes of the projectile have shorter range at the same velocity of the primary ion [13, 39]. Online PET was used for the first time clinically during the ^{12}C -ion pilot therapy project at GSI, Darmstadt, until 2008 [41], and a number of CPT centers are currently using PET for beam verification [32, 42–44], usually offline.

However, PET in C-ion therapy remains marginal and not really able to reduce range uncertainty as desired. The half-life of the most abundant induced radionuclides is too long for instantaneous feedback (Table 1), and the short-lived radionuclides are produced at a very low rate and exhibit a long positron range [45]. The measured activity is not directly correlated to the Bragg curve in phantoms (Figure 2), and the situation is worsened *in vivo* by the biological washout [43, 46]. An example comes from recent experiments on heavy-ion treatment of heart arrhythmia in a swine model, where online PET was used for range verification of a C-ion beam [47]. In Figure 3, we compare online to offline PET in a pig heart ventricular target irradiated with ^{12}C -ions. After 20 min, only the signal in the ribs is still visible in PET. The lack of a direct correlation with the dose (Figure 2) and the washout (Figure 3) makes resorting to Monte Carlo (MC) simulations [40] or other analytical calculations [48] currently unavoidable for data analysis. Furthermore, the activity is time-dependent according to the half-lives of the isotopes (Table 1) and the efficiency of the detector system in measuring the activity distribution. All these corrections currently limit the accuracy of PET-based range verification to about 2–5 mm [33, 42, 49].

RIB IN RADIOTHERAPY

The rationale for using RIB in therapy has looked in two directions. On one side, it was assumed that the radioactive decay can increase the dose in the target. This was similar to the rationale for using antiprotons [50] or pions [51] for therapy. Among radioactive isotopes, ^9C attracted attention because of its β -delayed decay in low-energy, densely ionizing particles [52]. However, despite some successful *in vitro* experiments [53], these approaches have been abandoned. The energy released by nuclear reaction in the target is indeed in the order of the nuclear shell energies, and such energy is always very small compared to the electromagnetic energy loss of the particle in the tumor. In fact, simulations show that the putative increase due to nuclear reactions in the target is negligible [54].

On the other hand, RIB can be used for image-guided particle therapy. In fact, the best way to increase the signal intensity in online PET would be the use of β^+ emitters for treatment. Using RIB, every primary ion will decay, essentially only at the end of the range, with the decay time always much longer than the travel time in the accelerator and in the patient's body. RIB would improve the count rate $\sim 10 \times$ [55], reduce the shift between measured activity and dose (Figure 2), and mitigate the washout blur of the image (Figure 3) with short-lived isotopes and in-beam acquisition. Heavy ion therapy is nowadays only performed using carbon ions, because with heavier ions, the toxicity in normal tissues can be unacceptable. The Heidelberg Ion Therapy (HIT) center is currently planning to use oxygen ions for radioresistant tumors, and therefore looking at Table 1, one should consider isotopes of C, N, and O as potential projectiles in RIB therapy.

The idea of using RIB in therapy is certainly not new, as the potential advantage in terms of improved precision and accuracy

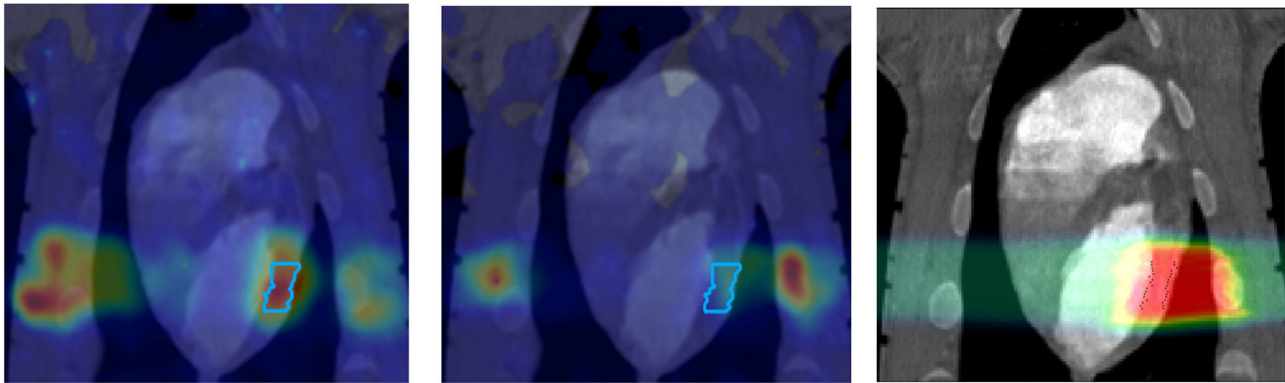


FIGURE 3 | PET images of a pig heart treated with ^{12}C -ions. The ventricular target is drawn in the treatment planning image overlaid to the CT (**Right**). Online PET image (**Left**) was acquired during the treatment at GSI, while the offline (center) was registered 20 min after the treatment. PET imaging obtained with the online PET camera at GSI, courtesy of Helmholtzzentrum Dresden (HZDR); details in Ref. [47].

was clear since the beginning of CPT. Below, we will describe past efforts in this direction.

Lawrence Berkeley Laboratory

Cancer therapy using ions heavier than protons was first tested in the pilot project of the Lawrence Berkeley Laboratory (LBL) in USA led by Cornelius A. Tobias. The project started in 1975 and used He, C, Ne, Si, and Ar ions, treating 1,314 patients until the shutdown of the Bevalac accelerator in 1992 [56, 57]. The uncertainty in predicting the correct range of heavy ions from the CT images, produced by X-rays, was soon clear and the LBL physicists explored the possibility of using RIB for range verification [58]. The LBL studies focused on ^{19}Ne (**Table 1**) and built a modified PET detector (PEBA) consisting of two arrays of 64 BiGe scintillators in an 8×8 matrix arrangement, which are separated by a distance of ~ 1 m (**Figure 4**). PEBA was already able to demonstrate an accuracy of ~ 1 mm in range determination in phantoms [21].

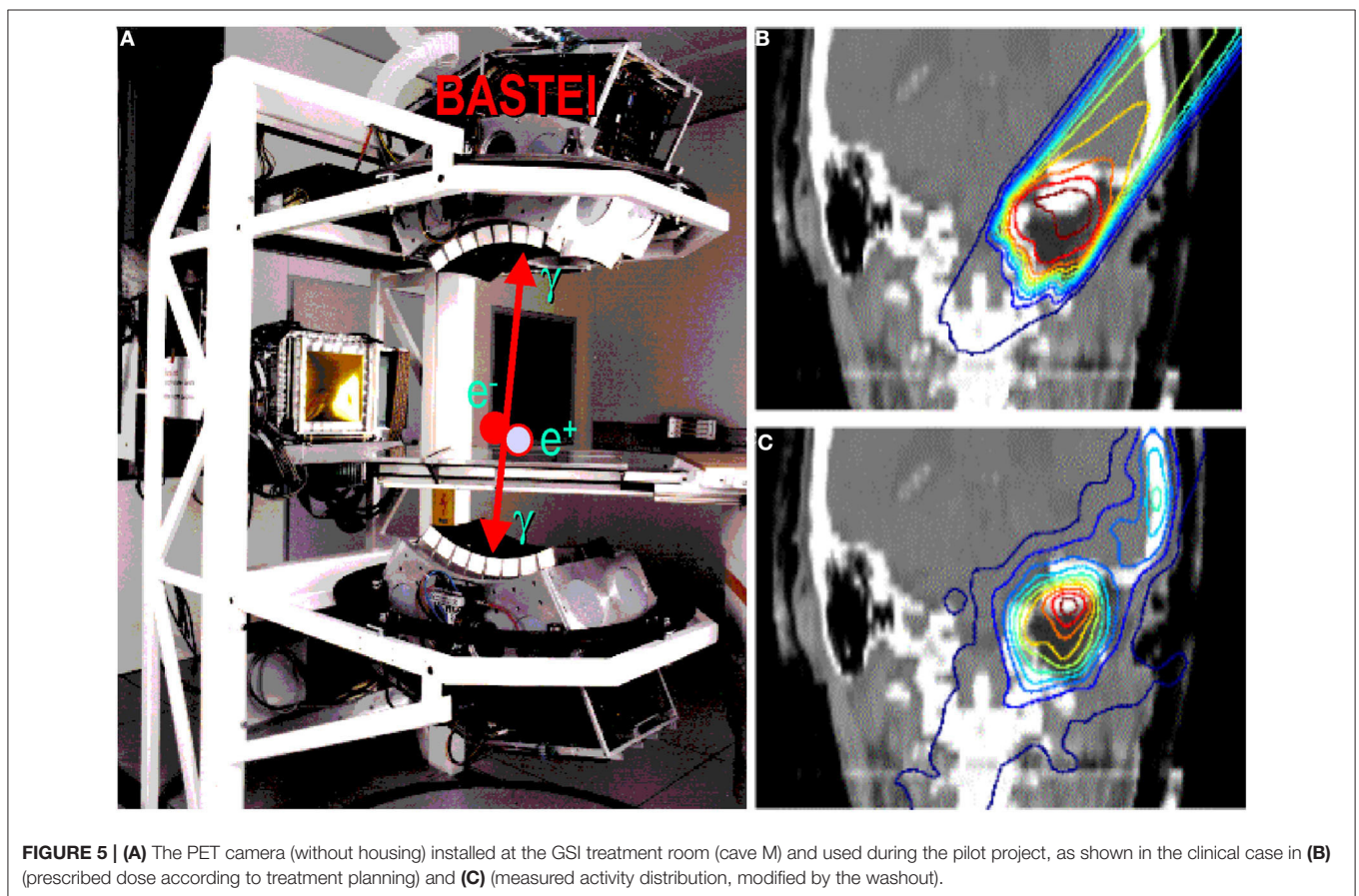
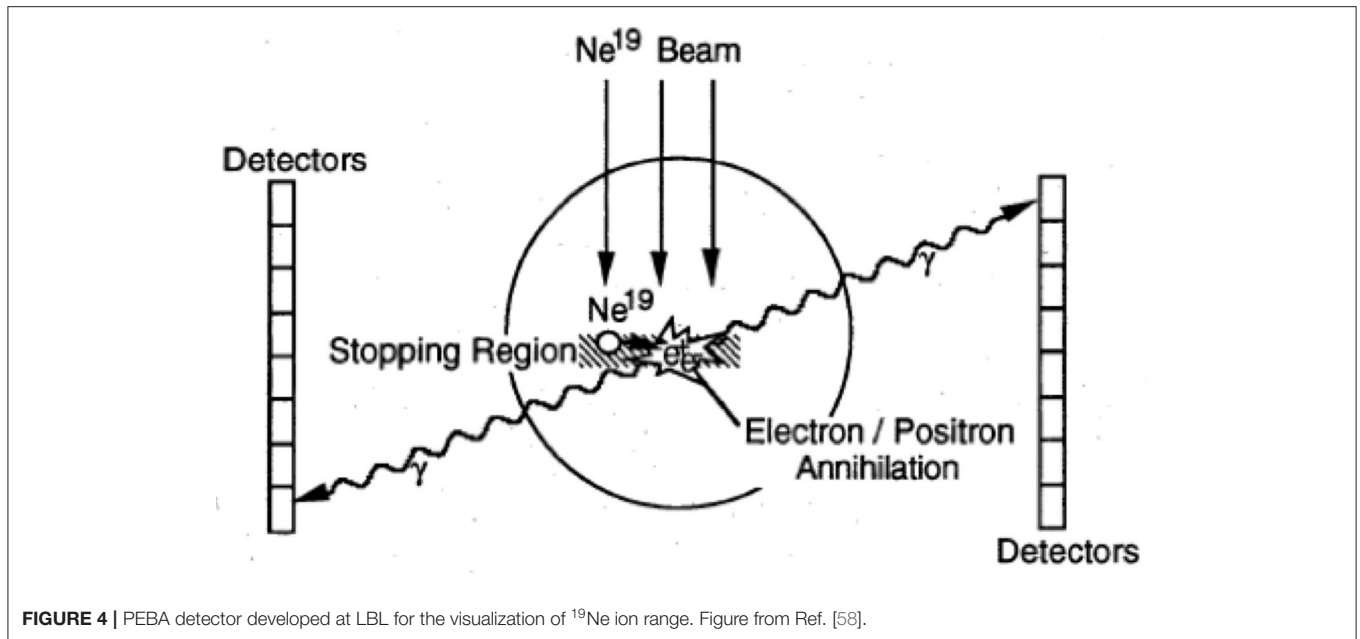
Eulima

The European Light Ion Medical Accelerator (EULIMA) project was funded by EU within the 2nd Framework Program in 1989. The project was led by the cyclotron laboratory in Nice, which was already active in proton therapy for eye treatment [59]. The concerted action studied the feasibility of a hospital-based light ion ($2 \leq z \leq 10$) accelerator facility for the treatment of a large number of cancer patients in Europe. The project explored the idea of using a superconducting cyclotron, based on the experience in Nice, and carefully analyzed the option of irradiating the patients with radioactive isotopes of carbon, oxygen, or neon. Cyclotrons have the advantage of high intensity and simplicity of operation. However, superconducting cyclotrons for ions as heavy as carbon requires an intense R&D for magnetic field shaping and high voltage. Synchrotrons are instead flexible machines, energy can be rapidly changed, different ion species can be accelerated, and they are a well-established technology. For these reasons, the EULIMA

feasibility study recommended using synchrotrons for heavy-ion therapy [60], and indeed all European ion beam centers are currently using synchrotrons. IBA, the leading company in cyclotrons for proton therapy, is still working on the idea of the superconducting cyclotron for carbon ions (C400) [61], in collaboration with GANIL at Caen (France), but the project is still ongoing.

GSI

The GSI Helmholtz Center for Heavy Ion Research in Darmstadt (Germany) treated the first patient in Europe with ions heavier than protons—carbon ions. The program was led by Gerhard Kraft and treated 440 patients with ^{12}C -ions between 1997 and 2008 [5, 62]. As noted in section Range Verification in Particle Therapy, the pilot project at GSI used for the first time PET online to verify the dose delivery (**Figure 5**). The group from Helmholtz Center Dresden that worked on the PET system also measured RIB, produced at the GSI fragment separator (FRS) [63]. They used ^{15}O , ^{17}F , and ^{19}Ne for testing the PET camera [64]. All patients in the pilot project were, however, treated with stable ^{12}C ions and PET images exploited mostly the ^{11}C projectile fragment produced by nuclear fragmentation. As shown in **Figure 3**, the same PET camera was recently used for irradiation of AV nodes and ventricles in swine hearts at GSI [47]. Radiotherapy for treatment of heart arrhythmia is considered a very promising non-invasive alternative to catheter ablation [65], and recent results with stereotactic radiosurgery for ventricular arrhythmia are very encouraging [66]. Charged particles are potentially much more effective for these kinds of treatment [67] because they require single high doses, and with X-rays, this can cause severe toxicity in the normal heart and other surrounding critical structures such as esophagus and lungs. However, the cardiac targets are small and rapidly moving, and therefore PET imaging plays a very important role for applications of heavy ions in non-cancer diseases. The first patient with ventricular arrhythmia has been treated with protons at CNAO (Pavia, Italy) in December 2019 [68].



HIMAC

Certainly, the accelerator facility that has the longest history and success in RIB production and testing for cancer therapy

is the HIMAC at NIRS in Chiba, Japan. Following the LBL pilot project, NIRS was the first center to treat patients with ions heavier than protons, specifically carbon ions.

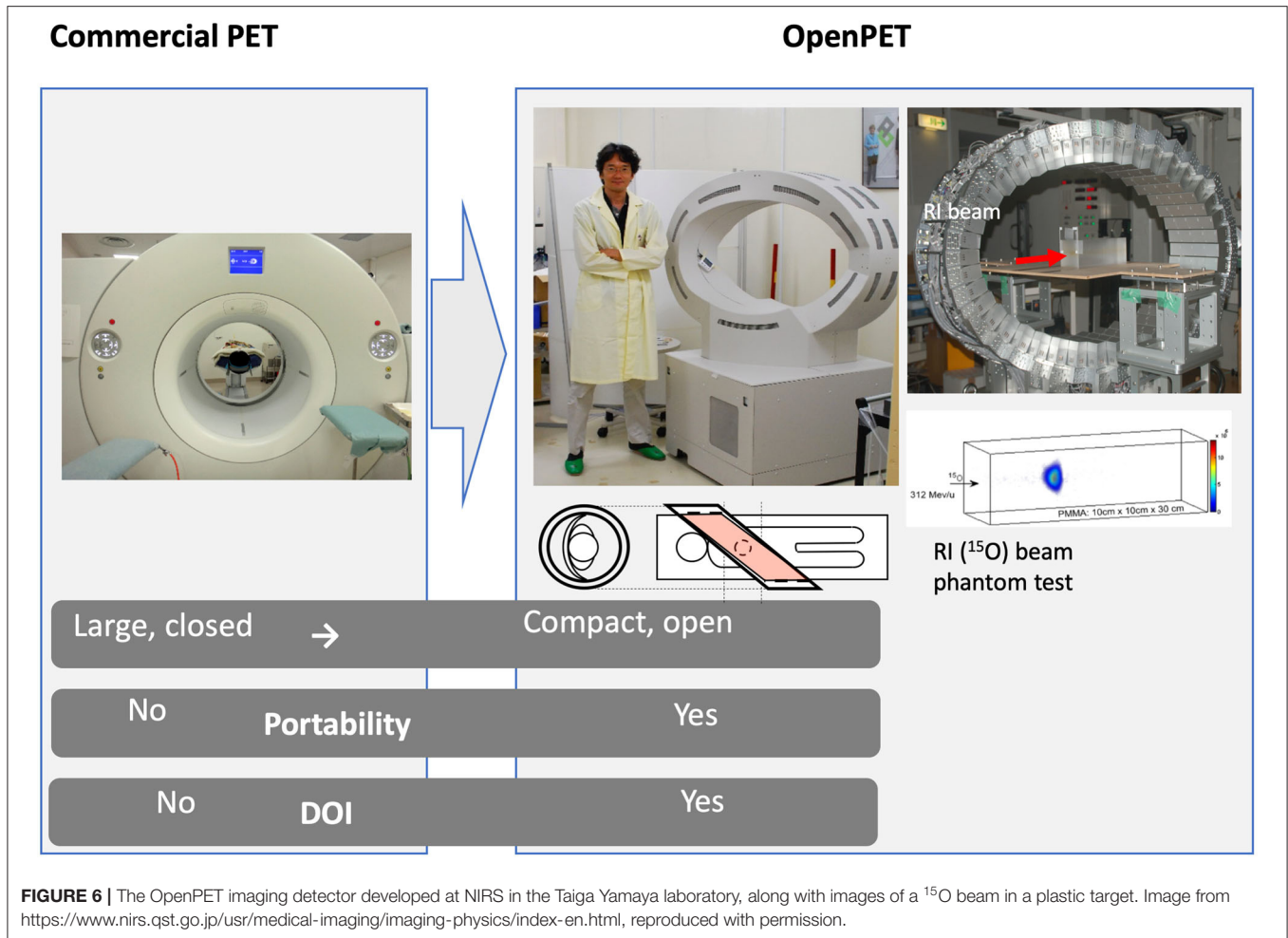


FIGURE 6 | The OpenPET imaging detector developed at NIRS in the Taiga Yamaya laboratory, along with images of a ¹⁵O beam in a plastic target. Image from <https://www.nirs.qst.go.jp/usr/medical-imaging/imaging-physics/index-en.html>, reproduced with permission.

NIRS used the flexible and reliable HIMAC synchrotron for patient treatments and research [69], and most of the patients treated worldwide with C-ions were actually irradiated at HIMAC [6]. In over 20 years of clinical operation, NIRS has demonstrated excellent results in many tumor sites with acceptable toxicity, very often in hypofractionation [70]. NIRS has always invested in research and development in heavy ion therapy and has been studying RIB for therapy for 20 years [71]. Considering the low RIB intensity (see section RIB Production), NIRS physicists were trying to use the RIB beam at low intensity as a probe before application of the stable carbon therapeutic beam. The Yamaya laboratory at NIRS has developed a new concept of open-PET [72–74] (Figure 6) to visualize the beam and has applied the system to study the washout of radionuclides in animal targets [75, 76]. Optical beam imaging has also been recently used to visualize RIB at HIMAC [77]. The HIMAC studies demonstrate that RIB have similar radiobiological properties as stable isotopes of the same atomic number but produce far better quality images for range verification, with 5–11-fold improvements in the PET signal/noise ratio [78].

RIB PRODUCTION

The main hindrance to the full exploitation of RIB in cancer therapy is the low intensity. RIB are a very important modern topic in nuclear physics, as they allow to study the properties of nuclear matter far from the stability curve [79]. To produce RIB, two techniques are used at particle accelerators: Isotope-on-line (ISOL) and in-flight [80, 81] (Figure 7). ISOL is based on light-ion (usually ¹H or ²H)-induced spallation or fission of thick targets (Ta or U). The radioactive fragments are extracted from the thick target through thermal diffusion at high temperature, effused to an ion source to become singly charged ions and finally accelerated toward a target. RIB production for therapy has so far used the in-flight technique, where RIB are obtained by fragmentation of the stable primary beam in thin targets (usually in C or Be). The reaction fragments, ejected in the forward direction with almost the same speed as that of the incident beam, are magnetically separated and then transferred to the experimental vault. The RIB (*A*, *N*-1) intensity is therefore determined by the fragmentation cross section of the primary beam (*A*, *N*). As shown in Table 2, the production cross section

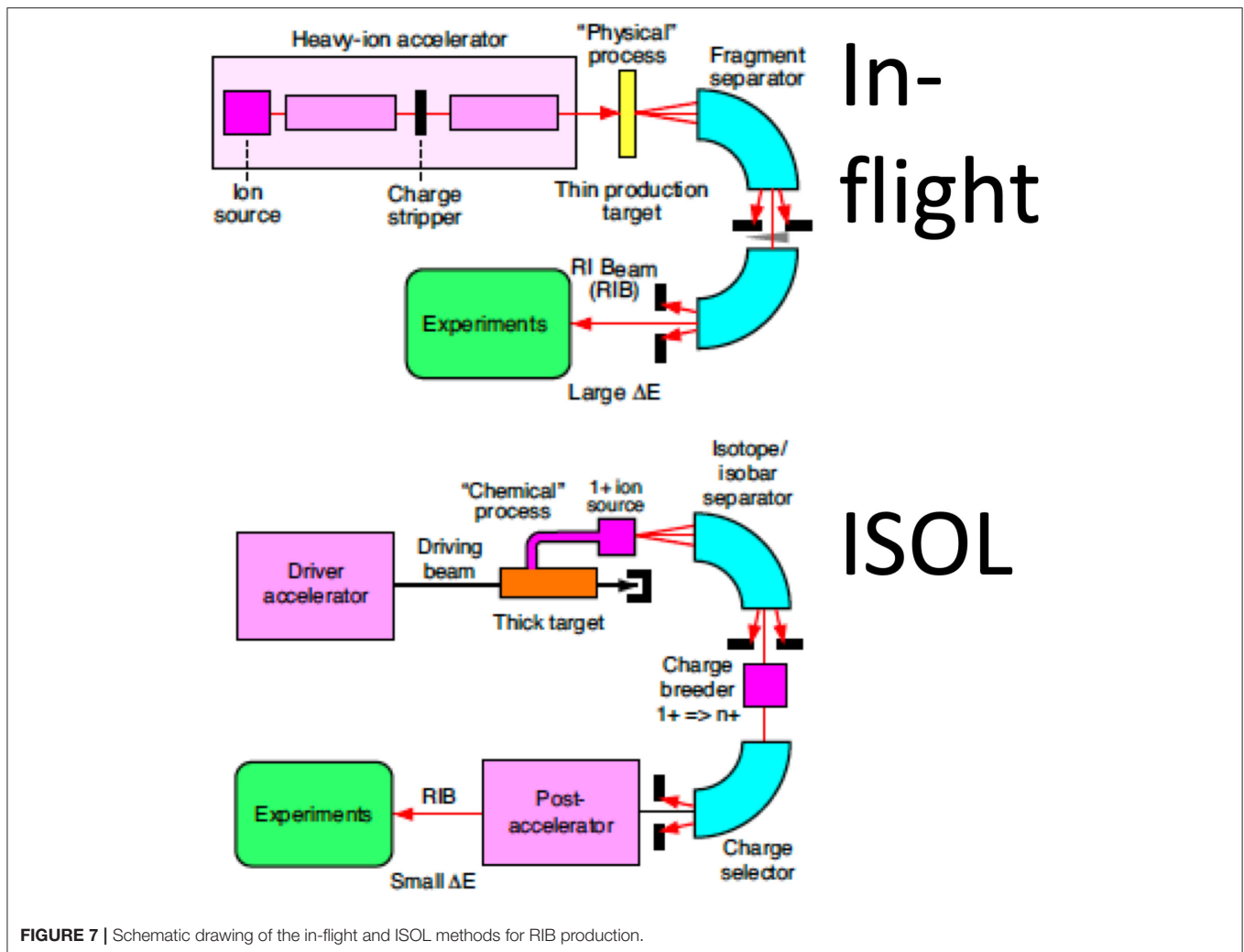


FIGURE 7 | Schematic drawing of the in-flight and ISOL methods for RIB production.

for light ions at high energy is ~ 45 mb per one nucleon, and decreases an order of magnitude for every further nucleon. Beam intensity is consequently reduced to $< 10^{-2}$ for $N-1$ isotopes and 10^{-3} for $N-2$ isotopes. At HIMAC, beams of ^{11}C were produced with intensities ranging 10^5 – 10^6 pps [77, 82], still too low for a therapeutic C-ion treatment that requires 10^8 – 10^9 pps [5, 13].

An additional problem in the in-flight technique is the large momentum spread. This spread causes a shift between the Bragg peak and activity peak for RIB [83]. Even if this shift is smaller than the one observed using stable ions for treatment and projectile fragments for PET imaging (Figure 2), it increases with the momentum acceptance. Recent measurements at HIMAC shows that for ^{11}C , the shift is around 2 mm at 5% acceptance and is reduced to 0.1 mm at 0.5% momentum acceptance [84]. Momentum spreads can therefore translate in significant range spreads at the site of stopping (Table 2).

In-flight production of RIB would be impractical in current medical synchrotrons. Already at LBL, it was hypothesized to produce the RIB at low energy and then inject them in the high-energy medical accelerator [21]. The idea is to build a small cyclotron that can produce low-energy RIB with an ISOL system,

and these ions are then injected in conventional synchrotrons. A source using low-energy electron beams for the production of ^{11}C has been designed and produced at HIMAC [85]. Within the MEDICIS-Promed project [86], CERN has proposed a charge breeding scheme based on an Electron Beam Ion Source for beam preparation of a radioactive ^{11}C beam [87]. The charge breeder is coupled to a medical synchrotron currently used for ^{12}C -ion therapy (such as MedAustron) to treat patients with ^{11}C using the same beam delivery devices of conventional heavy-ion therapy [88].

BARB

GSI-treated cancer patients with ^{12}C -ions accelerated at SIS, a 18 Tm synchrotron where the FRS has been used for many nuclear physics experiments [63]. SIS18 will be the injector of a new accelerator at 100 Tm, currently under construction for the Facility for Anti-protons and Ion Research (FAIR) [89] (Figure 8). A new FRS (super-FRS) will be built at SIS100 [90], to accommodate the ambitious physics program of the NuSTAR collaboration [91]. In addition to the nuclear

TABLE 2 | A MOCADI simulation of the RIB intensity at GSI FRS.

Primary beam	Intensity at SIS-18 (per cycle)	Secondary beams	Production cross-section (mb)	Intensity at FRS (pps)	Energy (MeV/n)	Range in water (cm)	Range straggling (cm)
^{12}C	8×10^{10}	^{10}C	4.8	2.3×10^7	334	17.2	0.4
		^{11}C	45.4	4.9×10^8	347	20.1	0.5
^{16}O	1×10^{11}	^{14}O	4.6	5.7×10^7	405	18.4	0.4
		^{15}O	45.6	9.1×10^8	416	20.6	0.4

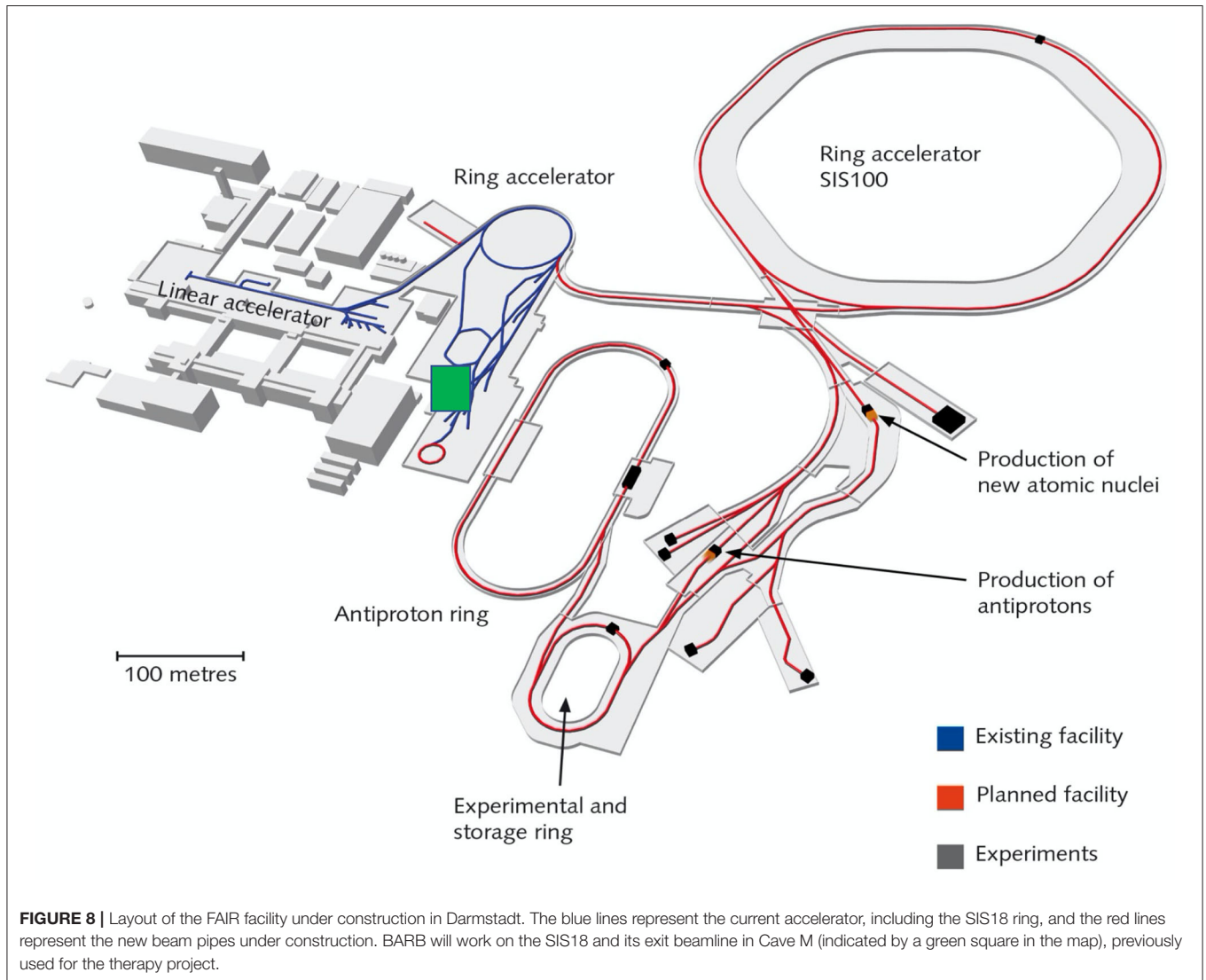
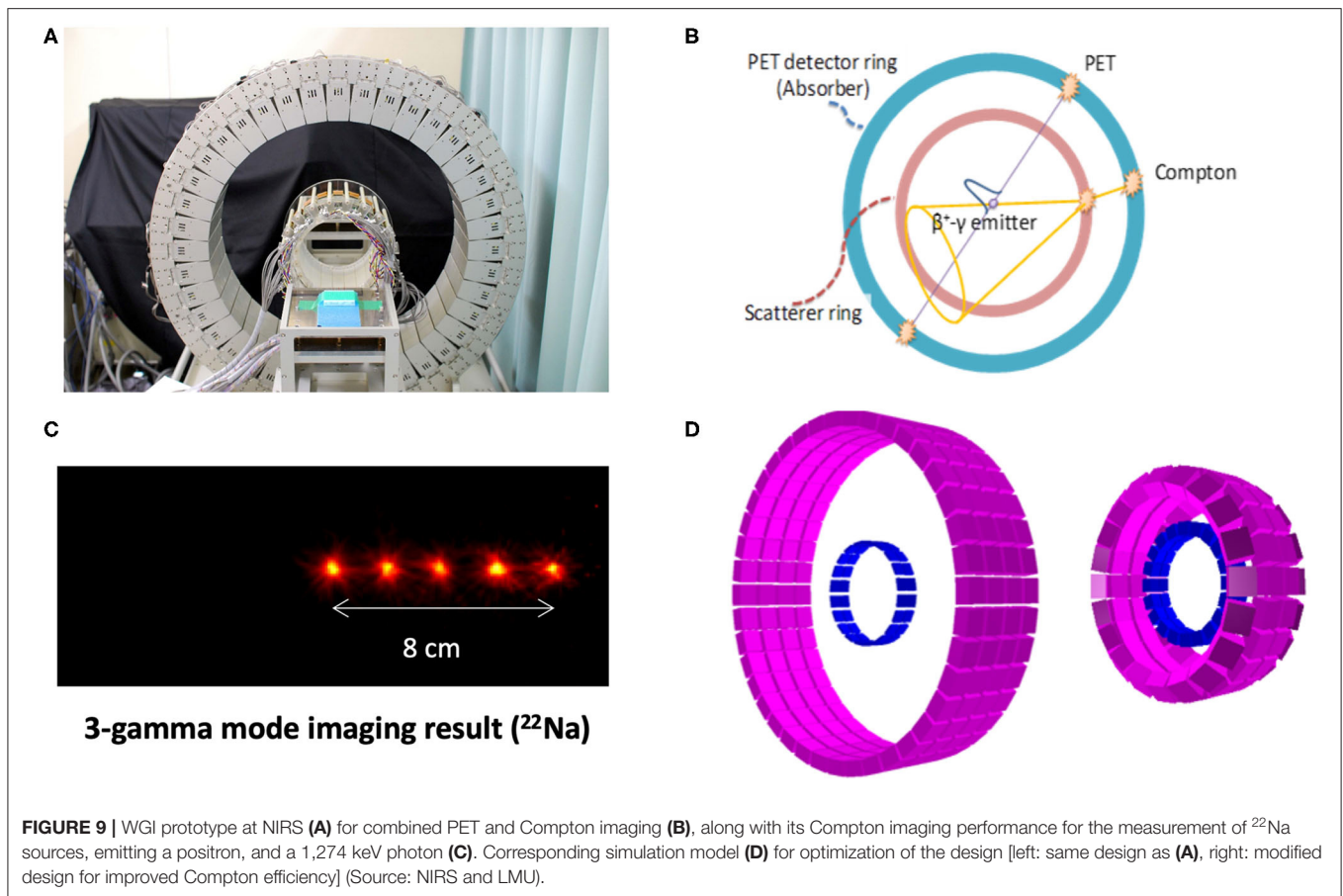


FIGURE 8 | Layout of the FAIR facility under construction in Darmstadt. The blue lines represent the current accelerator, including the SIS18 ring, and the red lines represent the new beam pipes under construction. BARB will work on the SIS18 and its exit beamline in Cave M (indicated by a green square in the map), previously used for the therapy project.

physics program, FAIR also includes a large applied physics program (APPA) in atomic physics, plasma physics, materials research, and biophysics [92]. The biophysics program at FAIR aims at exploiting the intensity and energy upgrades for therapy and space radiation protection research [93]. While SIS100 is under construction, the FAIR-phase-0 is already ongoing with the main goal of increasing the intensity by a factor of $\times 10,000$ compared to the current values [94].

The intensity upgrade at SIS18 can be exploited to test RIB therapy in the same Cave M (Figure 5) where the pilot project was performed. The project Biomedical Applications of Radioactive ion Beams (BARB) (www.gsi.de/BARB) aims at testing $^{10,11}\text{C}$ and $^{14,15}\text{O}$ for simultaneous treatment and imaging at FAIR, with the goal of reaching sub-mm precision in range verification and to demonstrate the potential of RIB therapy in an animal model. BARB is funded by EU within the 2019



ERC Advanced Grant call and is a 5-year project starting in late 2020.

FRS at FAIR

The radioactive ions of interest will be produced by fragmentation (one- or two-neutron removal, respectively) of relativistic primary beams (^{12}C , ^{16}O) in reaction targets (Be, C) placed at the entrance of the SIS18 FRS and separated in-flight [63]. As discussed in section RIB Production, the intensity of the RIB depends on the primary beam current, on the fragmentation cross-sections, and on the transport properties. **Table 2** gives the result of a Monte Carlo simulation with the GSI code MOCADI [95] using the intensities expected at SIS18 in FAIR-phase-0. The experimental activity in this task will focus on optimization of the accelerator parameters to reach the maximum intensities. The intensity in Cave M must be verified experimentally and critically depends on the size of the beam to be used for dosimetry and pre-clinical experiments in a mouse model. The MOCADI simulation indicates a range straggling $\sigma/R \sim 2.5\%$ for both light ions in the energy range of interest for therapy. The range straggling is a direct consequence of the momentum spread discussed in section RIB Production. Range straggling will therefore be carefully assessed during BARB in order to reach sub-millimeter precisions. It is also possible to apply methods to produce mono-energetic, pencil-like secondary

beams for therapy, e.g., using the energy-focusing method that was developed at the FRS [96].

Hybrid Detector

The second innovative aspect of BARB is the use of a new γ -PET detector that will be designed and built at LMU. Cave M is equipped with an online PET (**Figure 5**), but even online PET can only register in-between the synchrotron beam spills, because the signal is obscured by the large prompt γ -ray signal during the irradiation [72, 97]. An improved detector should be able to exploit the prompt γ -ray emission [23] during beam extraction, in addition to the PET acquisition (and concomitant third- γ emission in case of ^{10}C and ^{14}O) in-between the synchrotron spills. BARB will build a hybrid detector concept aiming to exploit both the prompt γ -rays emitted in nuclear interactions during the beam-on time of the synchrotron pulsed delivery, and the delayed emission of the $(\gamma^-)\beta^+$ -emitting primary beam (superimposed to a minor contribution of positron emitting projectile and target fragments) in the beam pauses [37]. The new detector concept will be based on an advanced version of the γ -PET design originally proposed at LMU [98] and further developed in the framework of the International Open Laboratory and International Research Initiative between LMU and NIRS (**Figure 9**). The focus of these joint NIRS-LMU efforts has been on the imaging of nuclear medicine tracers that undergo

β^+ -decay with simultaneous emission of a third prompt photon from the excited daughter nucleus, thus making it possible to achieve improved imaging performances by the intersection of the annihilation photons' line of response (LOR) and the third photon Compton cone [98]. A promising proof of concept of this so-called whole gamma imaging (WGI) [99] approach could be already demonstrated at NIRS in a mouse using ^{89}Zr , which has a β^+ and electron capture decay in $^{89\text{m}}\text{Y}$ with a half-life of 78 h. $^{89\text{m}}\text{Y}$ finally decays into the stable ^{89}Y by an emission of 909 keV γ -ray and a half-life of 15.7 s [100]. Hybrid PET, Compton, and Compton-PET imaging were obtained relying on the addition of a scatterer ring (94 mm diameter) made of GAGG scintillator crystals inside a full-size (660 mm diameter) PET scanner with depth-of-interaction Zr-doped GSO scintillator detectors already available at NIRS [101, 102]. While nuclear medicine tracer imaging is limited to single- γ energies up to ~ 1 MeV, the energy of interest of prompt- γ typically lies in the 3–8 MeV interval and is a priori unknown. Hence, recent research at LMU has focused on design studies aiming to upgrade the NIRS detector in terms of enhanced efficiency of Compton imaging at these higher PG energies, without compromising the PET imaging performance. The desired improvements, initially focused on applications to proton therapy [103], could be achieved by increasing the thickness of the scattering layer and decreasing the relative distances between the scatterer and absorber rings (Figure 9D). In the framework of BARB, these efforts will be tailored to RIB and benefit from the reduced fluence of heavy ions compared to protons at the same treatment dose, resulting in relaxed signal processing rate requirements [104]. Moreover, higher resolution detectors tailored to small animal imaging will likely be employed, as currently under development in a joint effort between LMU and NIRS for a novel small animal in-beam PET scanner being realized for the SIRMIO ERC Consolidator Grant [30]. All these optimization design studies largely benefited from the collaboration between LMU and the University of Berkeley, USA (BACATEC; <http://www.bacatec.de/>) which aimed at developing a powerful simulation and image reconstruction framework, including a machine-learning

algorithm for correct identification of the different types of event in the detectors [105]. Construction and detector testing for BARB will be performed in close collaboration between LMU and GSI groups.

CONCLUSIONS

For many years, RIB have been proposed as the ideal bullet for image-guided particle therapy. The main problem has been the production of RIB and the low beam intensity. Research in this field started already at LBL and is currently mostly driven by NIRS in Japan, with interesting results and design of innovative PET detectors. These problems can be overcome by future, high-intensity accelerators, or by injection of RIB in conventional synchrotrons. NIRS and CERN are studying RIB sources that can work with current medical synchrotrons. The practical advantage of RIB therapy compared to conventional stable-ion treatments remains, however, not demonstrated. This is the goal of the BARB project, currently ongoing at FAIR in collaboration with LMU in Germany. BARB will exploit the intensity upgrade in FAIR-phase-0 and a novel γ -PET detector for beam visualization. BARB, NIRS, and CERN results in the coming decade will clarify whether there is a role of RIB in cancer treatment.

AUTHOR CONTRIBUTIONS

Both authors collected the literature and wrote the paper.

FUNDING

This work was supported by ERC grant 883425 BARB.

ACKNOWLEDGMENTS

We thank Taiga Yamaya, Mohammad Safari, and Christian Graeff for providing some figures and for fruitful discussions. We are grateful to Christoph Scheidenberger for the MOCADI simulation in Table 2.

REFERENCES

- Lievens Y, Borras JM, Grau C. Provision and use of radiotherapy in Europe. *Mol Oncol.* (2020) 14:1461–9. doi: 10.1002/1878-0261.12690
- Jaffray DA. Image-guided radiotherapy: from current concept to future perspectives. *Nat Rev Clin Oncol.* (2012) 9:688–99. doi: 10.1038/nrclinonc.2012.194
- Grau C, Durante M, Georg D, Langendijk JA, Weber DC. Particle therapy in Europe. *Mol Oncol.* (2020) 14:1492–9. doi: 10.1002/1878-0261.12677
- Durante M, Orecchia R, Loeffler JS. Charged-particle therapy in cancer: clinical uses and future perspectives. *Nat Rev Clin Oncol.* (2017) 14:483–95. doi: 10.1038/nrclinonc.2017.30
- Schardt D, Elsässer T, Schulz-Ertner D. Heavy-ion tumor therapy: physical and radiobiological benefits. *Rev Mod Phys.* (2010) 82:383–425. doi: 10.1103/RevModPhys.82.383
- Tsujii H, Kamada T, Shirai T, Noda K, Tsujii H, Karasawa K, editors. *Carbon-Ion Radiotherapy*. Tokyo: Springer (2014). doi: 10.1007/978-4-431-54457-9
- Rackwitz T, Debus J. Clinical applications of proton and carbon ion therapy. *Semin Oncol.* (2019) 46:226–32. doi: 10.1053/j.seminonc.2019.07.005
- Durante M, Debus J. Heavy charged particles: does improved precision and higher biological effectiveness translate to better outcome in patients? *Semin Radiat Oncol.* (2018) 28:160–7. doi: 10.1016/j.semradonc.2017.11.004
- Bortfeld TR, Loeffler JS. Three ways to make proton therapy affordable. *Nature.* (2017) 549:451–3. doi: 10.1038/549451a
- Verma V, Mishra MV, Mehta MP. A systematic review of the cost and cost-effectiveness studies of proton radiotherapy. *Cancer.* (2016) 122:1483–501. doi: 10.1002/cncr.29882
- Farr JB, Flanz JB, Gerbershagen A, Moyers MF. New horizons in particle therapy systems. *Med Phys.* (2018) 45:e953–83. doi: 10.1002/mp.13193
- Noda K, Furukawa T, Fujisawa T, Iwata Y, Kanai T, Kanazawa M, et al. New accelerator facility for carbon-ion cancer-therapy. *J Radiat Res.* (2007) 48:A43–54. doi: 10.1269/jrr.48.A43
- Durante M, Paganetti H. Nuclear physics in particle therapy : a review. *Rep Prog Phys.* (2016) 79:096702. doi: 10.1088/0034-4885/79/9/096702
- Lomax AJ. Myths and realities of range uncertainty. *Br J Radiol.* (2020) 93:20190582. doi: 10.1259/bjr.20190582
- Bert C, Durante M. Motion in radiotherapy: particle therapy. *Phys Med Biol.* (2011) 56:R113–44. doi: 10.1088/0031-9155/56/16/R01

16. Pacelli R, Caroprese M, Palma G, Oliviero C, Clemente S, Cella L, et al. Technological evolution of radiation treatment: implications for clinical applications. *Semin Oncol.* (2019) 46:193–201. doi: 10.1053/j.seminoncol.2019.07.004
17. Bayouth JE, Low DA, Zaidi H. MRI-linac systems will replace conventional IGRT systems within 15 years. *Med Phys.* (2019) 46:3753–6. doi: 10.1002/mp.13657
18. Noble DJ, Burnet NG. The future of image-guided radiotherapy—is image everything? *Br J Radiol.* (2018) 91:20170894. doi: 10.1259/bjr.20170894
19. Paganetti H. Range uncertainties in proton therapy and the role of Monte Carlo simulations. *Phys Med Biol.* (2012) 57:R99–117. doi: 10.1088/0031-9155/57/11/R99
20. Durante M, Flanz J. Charged particle beams to cure cancer: Strengths and challenges. *Semin Oncol.* (2019) 46:219–25. doi: 10.1053/j.seminoncol.2019.07.007
21. Chu WT, Ludewigt BA, Renner TR. Instrumentation for treatment of cancer using proton and light ion beams. *Rev Sci Instrum.* (1993) 64:2055–122. doi: 10.1063/1.1143946
22. Cavaier RF, Haddad F, Sounalet T, Stora T, Zahi I. Terbium radionuclides for theranostics applications: a focus On MEDICIS-PROMED. *Phys Procedia.* (2017) 90:157–63. doi: 10.1016/j.phpro.2017.09.053
23. Krimmer J, Dauvergne D, Létang JM, Testa É. Prompt-gamma monitoring in hadrontherapy: a review. *Nucl Instruments Methods Phys Res Sect A.* (2018) 878:58–73. doi: 10.1016/j.nima.2017.07.063
24. Mattei I, Battistoni G, Bini F, Collamati F, De Lucia E, Durante M, et al. Prompt- γ production of 220 MeV/u 12C ions interacting with a PMMA target. *J Instrum.* (2015) 10:P10034. doi: 10.1088/1748-0221/10/10/P10034
25. Pinto M, Bajard M, Brons S, Chevallier M, Dauvergne D, Dedes G, et al. Absolute prompt-gamma yield measurements for ion beam therapy monitoring. *Phys Med Biol.* (2015) 60:565–94. doi: 10.1088/0031-9155/60/2/565
26. Lehrack S, Assmann W, Bertrand D, Henrotin S, Hérault J, Heymans V, et al. Submillimeter synchroacoustic range determination for protons in water at a clinical synrocyclotron. *Phys Med Biol.* (2017) 62:L20–30. doi: 10.1088/1361-6560/aa81f8
27. Mazzucconi D, Agosteo S, Ferrarini M, Fontana L, Lante V, Pullia M, et al. Mixed particle beam for simultaneous treatment and online range verification in carbon ion therapy: proof-of-concept study. *Med Phys.* (2018) 45:5234–43. doi: 10.1002/mp.13219
28. Piersanti L, Bellini F, Bini F, Collamati F, De Lucia E, Durante M, et al. Measurement of charged particle yields from PMMA irradiated by a 220 MeV/u 12C beam. *Phys Med Biol.* (2014) 59:1857–72. doi: 10.1088/0031-9155/59/7/1857
29. Félix-Bautista R, Gehrke T, Ghesquière-Diérickx L, Reimold M, Amato C, Turecek D, et al. Experimental verification of a non-invasive method to monitor the lateral pencil beam position in an anthropomorphic phantom for carbon-ion radiotherapy. *Phys Med Biol.* (2019) 64:175019. doi: 10.1088/1361-6560/ab2ca3
30. Parodi K, Assmann W, Belka C, Bortfeldt J, Clevert DA, Dedes G, et al. Towards a novel small animal proton irradiation platform: the SIRMIO project. *Acta Oncol.* (2019) 58:1470–5. doi: 10.1080/0284186X.2019.1630752
31. Traini G, Mattei I, Battistoni G, Bisogni MG, De Simoni M, Dong Y, et al. Review and performance of the dose profiler, a particle therapy treatments online monitor. *Phys Med Biol.* (2019) 65:84–93. doi: 10.1016/j.ejmp.2019.07.010
32. Ferrero V, Fiorina E, Morrocchi M, Pennazio F, Baroni G, Battistoni G, et al. Online proton therapy monitoring: clinical test of a Silicon-photodetector-based in-beam PET. *Sci Rep.* (2018) 8:4100. doi: 10.1038/s41598-018-22325-6
33. Knopf AC, Lomax A. *In vivo* proton range verification: a review. *Phys Med Biol.* (2013) 58:R131–60. doi: 10.1088/0031-9155/58/15/R131
34. Kraan AC. Range verification methods in particle therapy: underlying physics and monte carlo modeling. *Front Oncol.* (2015) 5:150. doi: 10.3389/fonc.2015.00150
35. Parodi K, Polf JC. *In vivo* range verification in particle therapy. *Med Phys.* (2018) 45:e1036–50. doi: 10.1002/mp.12960
36. Parodi K. Latest developments in *in-vivo* imaging for proton therapy. *Br J Radiol.* (2020) 93:20190787. doi: 10.1259/bjr.20190787
37. Parodi K. Vision 20/20: Positron emission tomography in radiation therapy planning, delivery, and monitoring. *Med Phys.* (2015) 42:7153–68. doi: 10.1118/1.4935869
38. Gambhir SS. Molecular imaging of cancer with positron emission tomography. *Nat Rev Cancer.* (2002) 2:683–93. doi: 10.1038/nrc882
39. Sommerer F, Cerutti F, Parodi K, Ferrari A, Enghardt W, Aiginger H. In-beam PET monitoring of mono-energetic 16 O and 12 C beams: experiments and FLUKA simulations for homogeneous targets. *Phys Med Biol.* (2009) 54:3979–96. doi: 10.1088/0031-9155/54/13/003
40. Kraan AC, Battistoni G, Belcari N, Camarlinghi N, Cirrone GAP, Cuttone G, et al. Proton range monitoring with in-beam PET: Monte Carlo activity predictions and comparison with cyclotron data. *Phys Med Biol.* (2014) 30:559–69. doi: 10.1016/j.ejmp.2014.04.003
41. Enghardt W, Parodi K, Crespo P, Fiedler F, Pawelke J, Pönisch F. Dose quantification from in-beam positron emission tomography. *Radiother Oncol.* (2004) 73:S96–8. doi: 10.1016/S0167-8140(04)80024-0
42. Handrack J, Tessonier T, Chen W, Liebl J, Debus J, Bauer J, et al. Sensitivity of post treatment positron emission tomography/computed tomography to detect inter-fractional range variations in scanned ion beam therapy. *Acta Oncol.* (2017) 56:1451–8. doi: 10.1080/0284186X.2017.1348628
43. Bauer J, Unholtz D, Sommerer F, Kurz C, Haberer T, Herfarth K, et al. Implementation and initial clinical experience of offline PET/CT-based verification of scanned carbon ion treatment. *Radiother Oncol.* (2013) 107:218–26. doi: 10.1016/j.radonc.2013.02.018
44. Nishio T, Miyatake A, Ogino T, Nakagawa K, Saijo N, Esumi H. The development and clinical use of a beam ON-LINE PET system mounted on a rotating gantry port in proton therapy. *Int J Radiat Oncol.* (2010) 76:277–86. doi: 10.1016/j.ijrobp.2009.05.065
45. Buitenhuis HJT, Diblen F, Brzezinski KW, Brandenburg S, Dendooven P. Beam-on imaging of short-lived positron emitters during proton therapy. *Phys Med Biol.* (2017) 62:4654–72. doi: 10.1088/1361-6560/aa6b8c
46. Ammar C, Frey K, Bauer J, Melzig C, Chiblak S, Hildebrandt M, et al. Comparing the biological washout of $\beta +$ -activity induced in mice brain after 12 C-ion and proton irradiation. *Phys Med Biol.* (2014) 59:7229–44. doi: 10.1088/0031-9155/59/23/7229
47. Lehmann HI, Graeff C, Simoniello P, Constantinescu A, Takami M, Lugeniel P, et al. Feasibility study on cardiac arrhythmia ablation using high-energy heavy ion beams. *Sci Rep.* (2016) 6:38895. doi: 10.1038/srep38895
48. Pinto M, Kroeniger K, Bauer J, Nilsson R, Traneus E, Parodi K. A filtering approach for PET and PG predictions in a proton treatment planning system. *Phys Med Biol.* (2020) 65:095014. doi: 10.1088/1361-6560/ab8146
49. Nischwitz SP, Bauer J, Welzel T, Rief H, Jäkel O, Haberer T, et al. Clinical implementation and range evaluation of *in vivo* PET dosimetry for particle irradiation in patients with primary glioma. *Radiother Oncol.* (2015) 115:179–85. doi: 10.1016/j.radonc.2015.03.022
50. Bassler N, Alsner J, Beyer G, DeMarco JJ, Doser M, Hajdukovic D, et al. Antiproton radiotherapy. *Radiother Oncol.* (2008) 86:14–9. doi: 10.1016/j.radonc.2007.11.028
51. Bagshaw MA, Li GC, Pistenma DA, Fessenden P, Luxton G, Hoffmann WW. Introduction to the use of negative pi-mesons in radiation therapy: Rutherford 1964, revisited. *Int J Radiat Oncol.* (1977) 3:287–92. doi: 10.1016/0360-3016(77)90266-8
52. Li Q, Kanai T, Kitagawa A. The potential application of β -delayed particle decay beam 9C in cancer therapy. *Phys Med Biol.* (2004) 49:1817–31. doi: 10.1088/0031-9155/49/9/016
53. Li Q, Furusawa Y, Kanazawa M, Kanai T, Kitagawa A, Aoki M, et al. Enhanced efficiency in cell killing at the penetration depths around the Bragg peak of a radioactive 9C-ion beam. *Int J Radiat Oncol.* (2005) 63:1237–44. doi: 10.1016/j.ijrobp.2005.08.006
54. Mancusi D, Sihver L, Niita K, Li Q, Sato T, Iwase H, et al. Calculation of energy-deposition distributions and microdosimetric estimation of the biological effect of a 9C beam. *Radiat Environ Biophys.* (2009) 48:135–43. doi: 10.1007/s00411-008-0206-8
55. Augusto RS, Bauer J, Bouhali O, Cuccagna C, Gianoli C, Kozłowska WS, et al. An overview of recent developments in FLUKA PET tools. *Phys Med Biol.* (2018) 54:189–99. doi: 10.1016/j.ejmp.2018.06.636

56. Castro JR. Results of heavy ion radiotherapy. *Radiat Environ Biophys.* (1995) 34:45–8. doi: 10.1007/BF01210545
57. Castro JR, Saunders WM, Tobias CA, Chen GTY, Curtis S, Lyman JT, et al. Treatment of cancer with heavy charged particles. *Int J Radiat Oncol Biol Phys.* (1982) 8:2191–8. doi: 10.1016/0360-3016(82)90569-7
58. Llacer J, Chatterjee A, Alpen EL, Saunders W, Andreae S, Jackson HC. Imaging by injection of accelerated radioactive particle beams. *IEEE Trans Med Imaging.* (1984) 3:80–90. doi: 10.1109/TMI.1984.4307660
59. Dendale R, Thariat J, Doyen J, Balosso J, Stefan D, Bolle S, et al. État des lieux de la protonthérapie en France en 2019. *Cancer/Radiothérapie.* (2019) 23:617–24. doi: 10.1016/j.canrad.2019.07.129
60. Mandrillon P, Farley FJM, Tang JY, Carli C, Cesari G, Fiétier N, et al. Feasibility studies of the EULIMA light ion medical accelerator. In: *3rd European Particle Accelerator Conference.* Berlin (1992). p. 179–191. Available online at: <http://infoscience.epfl.ch/record/104653>
61. Jongen Y, Abs M, Blondin A, Kleevan W, Zarembo S, Vandeplassche D, et al. Compact superconducting cyclotron C400 for hadron therapy. *Nucl Instruments Methods Phys Res Sect A.* (2010) 624:47–53. doi: 10.1016/j.nima.2010.09.028
62. Amaldi U, Kraft G. Radiotherapy with beams of carbon ions. *Reports Prog Phys.* (2005) 68:1861–82. doi: 10.1088/0034-4885/68/8/R04
63. Geissel H, Armbruster P, Behr KH, Brünle A, Burkard K, Chen M, et al. The GSI projectile fragment separator (FRS): a versatile magnetic system for relativistic heavy ions. *Nucl Instruments Methods Phys Res Sect B.* (1992) 70:286–97. doi: 10.1016/0168-583X(92)95944-M
64. Pawelke J, Byars L, Enghardt W, Fromm WD, Geissel H, Hasch BG, et al. The investigation of different cameras for in-beam PET imaging. *Phys Med Biol.* (1996) 41:279–96. doi: 10.1088/0031-9155/41/2/006
65. van der Ree MH, Blanck O, Limpens J, Lee CH, Balgobind BV, Dieleman EMT, et al. 'Cardiac Radioablation – a Systematic Review'. *Hear Rhythm.* (2020) 17:P1381–92. doi: 10.1016/j.hrthm.2020.03.013
66. Cuculich PS, Schill MR, Kashani R, Mutic S, Lang A, Cooper D, et al. Noninvasive cardiac radiation for ablation of ventricular tachycardia. *N Engl J Med.* (2017) 377:2325–36. doi: 10.1056/NEJMoa1613773
67. Bert C, Engenhart-Cabillic R, Durante M. Particle therapy for noncancer diseases. *Med Phys.* (2012) 39:1716–27. doi: 10.1118/1.3691903
68. Dusi V, Russo G, Forte GI, De Ferrari GM. Non-invasive ablation of cardiac arrhythmia. Is proton radiation therapy a step forward? *Int J Cardiol.* (2020) 316:64–6. doi: 10.1016/j.ijcard.2020.04.035
69. Murakami T, Tsujii H, Furusawa Y, Ando K, Kanai T, Yamada S, et al. Medical and other applications of high-energy heavy-ion beams from HIMAC. *J Nucl Mater.* (1997) 248:360–8. doi: 10.1016/S0022-3115(97)00135-9
70. Kamada T, Tsujii H, Blakely EA, Debus J, De Neve W, Durante M, et al. Carbon ion radiotherapy in Japan: an assessment of 20 years of clinical experience. *Lancet Oncol.* (2015) 16:e93–100. doi: 10.1016/S1470-2045(14)70412-7
71. Kanazawa M, Kitagawa A, Kouda S, Nishio T, Torikoshi M, Noda K, et al. Application of an RI-beam for cancer therapy: *In-vivo* verification of the ion-beam range by means of positron imaging. *Nucl Phys A.* (2002) 701:244–52. doi: 10.1016/S0375-9474(01)01592-5
72. Hirano Y, Yoshida E, Kinouchi S, Nishikido F, Inadma N, Murayama H, et al. Monte Carlo simulation of small OpenPET prototype with 11 C beam irradiation: effects of secondary particles on in-beam imaging. *Phys Med Biol.* (2014) 59:1623–40. doi: 10.1088/0031-9155/59/7/1623
73. Sakurai H, Itoh F, Hirano Y, Nitta M, Suzuki K, Kato D, et al. Positron annihilation spectroscopy of biological tissue in ¹¹C irradiation. *Phys Med Biol.* (2014) 59:7031–8. doi: 10.1088/0031-9155/59/22/7031
74. Mohammadi A, Yoshida E, Tashima H, Nishikido F, Inaniwa T, Kitagawa A, et al. Production of an 15 O beam using a stable oxygen ion beam for in-beam PET imaging. *Nucl Instruments Methods Phys Res Sect A.* (2017) 849:76–82. doi: 10.1016/j.nima.2016.12.028
75. Hirano Y, Takuwa H, Yoshida E, Nishikido F, Nakajima Y, Wakizaka H, et al. Washout rate in rat brain irradiated by a 11 C beam after acetazolamide loading using a small single-ring OpenPET prototype. *Phys Med Biol.* (2016) 61:1875–87. doi: 10.1088/0031-9155/61/5/1875
76. Toramatsu C, Yoshida E, Wakizaka H, Mohammadi A, Ikoma Y, Tashima H, et al. Washout effect in rabbit brain: in-beam PET measurements using 10 C, 11 C and 15 O ion beams. *Biomed Phys Eng Express.* (2018) 4:035001. doi: 10.1088/2057-1976/aaade7
77. Kang HG, Yamamoto S, Takyu S, Nishikido F, Mohammadi A, Horita R, et al. Optical imaging for the characterization of radioactive carbon and oxygen ion beams. *Phys Med Biol.* (2019) 64:115009. doi: 10.1088/1361-6560/ab1ccf
78. Chacon A, James B, Tran L, Guatelli S, Chartier L, Prokopovich D, et al. Experimental investigation of the characteristics of radioactive beams for heavy ion therapy. *Med Phys.* (2020) 47:3123–32. doi: 10.1002/mp.14177
79. Henning WF. Physics with energetic radioactive ion beams. *Nucl Instruments Methods Phys Res Sect B.* (1997) 126:1–6. doi: 10.1016/S0168-583X(97)00999-3
80. Raabe R. Making radioactive ion beams - Detecting reaction products. *Eur Phys J Plus.* (2016) 131:362. doi: 10.1140/epjp/i2016-16362-5
81. Blumenfeld Y, Nilsson T, Van Duppen P. Facilities and methods for radioactive ion beam production. *Phys Scr.* (2013) T152:014023. doi: 10.1088/0031-8949/2013/T152/014023
82. Iseki Y, Kanai T, Kanazawa M, Kitagawa A, Mizuno H, Tomitani T, et al. Range verification system using positron emitting beams for heavy-ion radiotherapy. *Phys Med Biol.* (2004) 49:3179–95. doi: 10.1088/0031-9155/49/14/012
83. Mohammadi A, Tashima H, Iwao Y, Takyu S, Akamatsu G, Nishikido F, et al. Range verification of radioactive ion beams of 11C and 15O using in-beam PET imaging. *Phys Med Biol.* (2019) 64:145014. doi: 10.1088/1361-6560/ab25ce
84. Mohammadi A, Tashima H, Iwao Y, Takyu S, Akamatsu G, Kang HG, et al. Influence of momentum acceptance on range monitoring of 11C and 15O ion beams using in-beam PET. *Phys Med Biol.* (2020) 65:125006. doi: 10.1088/1361-6560/ab8059
85. Katagiri K, Noda A, Nagatsu K, Nakao M, Hojo S, Muramatsu M, et al. A singly charged ion source for radioactive 11 C ion acceleration. *Rev Sci Instrum.* (2016) 87:02B509. doi: 10.1063/1.4935899
86. dos Santos Augusto R, Buehler L, Lawson S, Marzari S, Stachura M, Stora T, et al. CERN-MEDICIS (Medical Isotopes Collected from ISOLDE): a new facility. *Appl Sci.* (2014) 4:265–81. doi: 10.3390/app4020265
87. Pitters J, Breitenfeldt M, Pahl H, Pikin A, Wenander F. Summary of charge breeding investigations for a future 11C treatment facility. *CERN Acceler Sci.* (2018).
88. Stora T, Wenander F, Pitters J, Cocolios T, Stagemann S, Augusto R, et al. Technical design report for a carbon-11 treatment facility. *MEDICIS Promed.* (2019). Available online at: https://indico.cern.ch/event/782482/contributions/3396488/attachments/1837112/3010836/TDR_11C_Treatment_Facility-Erice_v1--6.pdf
89. Durante M, Indelicato P, Jonson B, Koch V, Langanke K, Meißner UG, et al. All the fun of the FAIR: fundamental physics at the facility for antiproton and ion research. *Phys Scr.* (2019) 94:033001. doi: 10.1088/1402-4896/aa9f3f
90. Winkler M, Geissel H, Weick H, Achenbach B, Behr KH, Boutin D, et al. The status of the super-FRS in-flight facility at FAIR. *Nucl Instruments Methods Phys Res Sect B.* (2008) 266:4183–7. doi: 10.1016/j.nimb.2008.05.073
91. Nilsson T. Radioactive ion beams at FAIR-NuSTAR. *Eur Phys J Spec Top.* (2008) 156:1–12. doi: 10.1140/epjst/e2008-00606-2
92. Stöhlker T, Bagnoud V, Blaum K, Blazevic A, Bräuning-Demian A, Durante M, et al. APPA at FAIR: from fundamental to applied research. *Nucl Instruments Methods Phys Res Sect B.* (2015) 365:680–5. doi: 10.1016/j.nimb.2015.07.077
93. Durante M, Golubev A, Park WY, Trautmann C. Applied nuclear physics at the new high-energy particle accelerator facilities. *Phys Rep.* (2019) 800:1–37. doi: 10.1016/j.physrep.2019.01.004
94. Bai M, Adonin A, Appel S, Bär R, Blell U, Bellachioma C, et al. Challenges of FAIR-phase-0. In: *9th International Particle Accelerator Conference.* Vancouver, BC: JACoW Publishing (2018). p. 2947–9.
95. Iwasa N, Weick H, Geissel H. New features of the Monte-Carlo code MOCADI. *Nucl Instruments Methods Phys Res Sect B.* (2011) 269:752–8. doi: 10.1016/j.nimb.2011.02.007
96. Scheidenberger C, Geissel H, Maier M, Münzenberg G, Portillo M, Savard G, et al. Energy and range focusing of in-flight separated exotic nuclei – A study for the energy-buncher stage of the low-energy branch of the Super-FRS. *Nucl Instruments Methods Phys Res Sect B.* (2003) 204:119–23. doi: 10.1016/S0168-583X(02)01898-0

97. Parodi K, Crespo P, Eickhoff H, Haberer T, Pawelke J, Schardt D, et al. Random coincidences during in-beam PET measurements at microbunched therapeutic ion beams. *Nucl Instruments Methods Phys Res Sect A*. (2005) 545:446–58. doi: 10.1016/j.nima.2005.02.002
98. Lang C, Habs D, Parodi K, Thirof PG. Sub-millimeter nuclear medical imaging with high sensitivity in positron emission tomography using $\beta + \gamma$ coincidences. *J Instrum*. (2014) 9:P01008. doi: 10.1088/1748-0221/9/01/P01008
99. Yamaya T, Yoshida E, Tashima H, Tsuji A, Nagatsu K, Yamaguchi M, et al. Whole gamma imaging (WGI) concept: simulation study of triple-gamma imaging. *J Nucl Med*. (2017) 58:152. doi: 10.1088/1361-6560/a/b8e89
100. Deri MA, Zeglis BM, Francesconi LC, Lewis JS. PET imaging with ^{89}Zr : from radiochemistry to the clinic. *Nucl Med Biol*. (2013) 40:3–14. doi: 10.1016/j.nucmedbio.2012.08.004
101. Tashima H, Yoshida E, Wakizaka H, Takahashi M, Nagatsu K, Tsuji A, et al. First ^{89}Zr mouse demonstration of whole gamma imaging (WGI). *J Nucl Med*. (2019) 60:196.
102. Tashima H, Yoshida E, Okumura Y, Suga M, Kawachi N, Kamada K, et al. Whole gamma imaging: demonstration of the $\beta + \gamma$ coincidence. In: *117th Scientific Meeting of the Japan Society of Medical Physics*. Yokohama (2019).
103. Safari M, Zoglauer A, Lovatti G, Anagnostatou V, Nitta M, Tashima H, et al. Performance of a novel hybrid gamma-imaging technique toward future 3D reconstruction of proton beam range. In: *IEEE Medical Imaging Conference*. Manchester (2019).
104. Safari M, Dedes G, Thirof P, Zoglauer A, Yamaya T, Durante M, et al. “Toward hybrid γ -PET imaging of radioactive ion beams at FAIR,” In: *GSI Scientific Report*. Darmstadt (2019). p. 57.
105. Safari M, Zoglauer A, Lovatti G, Anagnostatou V, Nitta M, Tashima H, et al. Development of a novel simulation and image reconstruction toolkit for PET and PG. In: *European Association of Nuclear Medicine (EANM) Congress*. Barcelona (2019).

Conflict of Interest: The authors declare that the research was conducted in the absence of any commercial or financial relationships that could be construed as a potential conflict of interest.

Copyright © 2020 Durante and Parodi. This is an open-access article distributed under the terms of the Creative Commons Attribution License (CC BY). The use, distribution or reproduction in other forums is permitted, provided the original author(s) and the copyright owner(s) are credited and that the original publication in this journal is cited, in accordance with accepted academic practice. No use, distribution or reproduction is permitted which does not comply with these terms.